

## Molecular Physics

An International Journal at the Interface Between Chemistry and Physics

ISSN: (Print) (Online) Journal homepage: <https://www.tandfonline.com/loi/tmph20>


# Substituted hydrocarbon: a CCSD(T) and local vibrational mode investigation

Alexis Antoinette Ann Delgado, Daniel Sethio, Devin Matthews, Vytor Oliveira & Elfi Kraka


To cite this article: Alexis Antoinette Ann Delgado, Daniel Sethio, Devin Matthews, Vytor Oliveira & Elfi Kraka (2021) Substituted hydrocarbon: a CCSD(T) and local vibrational mode investigation, Molecular Physics, 119:21-22, e1970844, DOI: [10.1080/00268976.2021.1970844](https://doi.org/10.1080/00268976.2021.1970844)

To link to this article: <https://doi.org/10.1080/00268976.2021.1970844>

 View supplementary material 

 Published online: 26 Aug 2021.





 Submit your article to this journal 

 Article views: 93

 View related articles 

 View Crossmark data 

## Substituted hydrocarbon: a CCSD(T) and local vibrational mode investigation

Alexis Antoinette Ann Delgado <sup>a</sup>, Daniel Sethio <sup>b</sup>, Devin Matthews <sup>a</sup>, Vytor Oliveira<sup>c</sup> and Elfi Kraka <sup>a</sup>

<sup>a</sup>Department of Chemistry, Southern Methodist University, Dallas, TX, USA; <sup>b</sup>Department of Chemistry – BMC, Uppsala University, Uppsala, Sweden; <sup>c</sup>Departamento de Química, Instituto Tecnológico de Aeronáutica (ITA), São José dos Campos, São Paulo, Brazil

### ABSTRACT

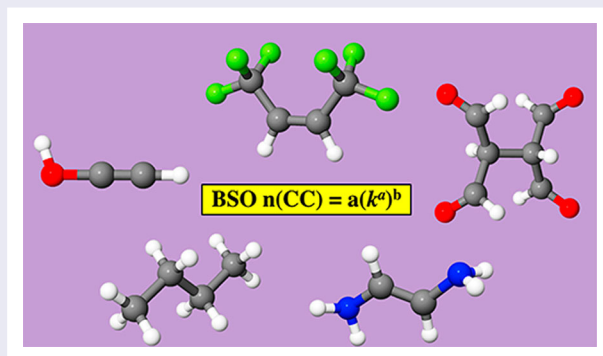
Substituent effects on the carbon–carbon bonds of hydrocarbons have been a topic of interest within the past seven decades as resultant information would enable one to tune the activity of CC bonds. However, current assessments of the  $C \equiv C$ ,  $C = C$ , and  $C - C$  bond strength of acetylene, ethylene, and ethane as well as their derivatives rely on indirect measures such as bond length and bond dissociation enthalpy. In this work, we introduce a quantitative measure of the intrinsic strength of  $C \equiv C$ ,  $C = C$ , and  $C - C$  bonds for a set of 40 hydrocarbon systems consisting of 3 parent structures, 36 hydrocarbon derivatives involving  $CF_3$ ,  $CH_3$ ,  $CHO$ ,  $F$ ,  $NH_2$ , or  $OH$  groups, and a conjugated system, based on vibrational spectroscopy. Local mode force constants  $k^a(CC)$  were computed at the CCSD(T)/cc-pVTZ level of theory for systems **1–32** and **34–40** and CCSD(T)/cc-pVDZ for **33**. From  $k^a(CC)$ , we derived related bond strength orders BSO  $n(CC)$  in order to provide quantitative measures of intrinsic bond strength. Topological electron density and natural population analyses were carried out as to analyze the nature of these bonds and complement bond strength measures. For substituted hydrocarbon systems, we found the strengthening/weakening of the CC bonds occurs as the covalent nature of the bond increases/decreases by means of varying charge delocalizations. Our findings provide new guidelines for desirably modulating  $C \equiv C$ ,  $C = C$ , and  $C - C$  bond strength and for the design of prospective pathways for bond cleavage reactions.

### ARTICLE HISTORY

Received 31 May 2021  
Accepted 7 August 2021

### KEYWORDS



Hydrocarbon derivatives; substitution effects; charge transfer; local vibrational mode analysis; intrinsic bond strength order




## 1. Introduction

Hydrocarbons represent the most basic class of organic molecules and remain predominant benefactors within petroleum [1,2], plastic [3,4], textile [5], and pharmaceutical industries [6]. Because such systems contain solely C and H atoms, which have a small electronegativity difference, their CC and CH bonds are largely non-polar.

Understanding the general framework of hydrocarbon systems has enabled chemists to devise effective methods for the cleavage of CC bonds in order to synthesise complex molecular architectures which are challenging to do otherwise. Typically, transition metals and ligands have been used to catalyse CC cleavage reactions via CC bond activation [7–13]. Determining how one could weaken

**CONTACT** Elfi Kraka  [ekraka@gmail.com](mailto:ekraka@gmail.com)  Department of Chemistry, Southern Methodist University, Dallas, 75275-0314 TX, USA  
A single table containing the atomic Cartesian coordinates for the molecules **1–40** are given in the Supporting Information.

 Supplemental data for this article can be accessed here. <https://doi.org/10.1080/00268976.2021.1970844>

CC bond would be beneficial towards this subject matter as the breakage of weakened CC bonds would require less energy.

Substitution with various functional groups can cause partial polarisation ( $\delta^+$ ,  $\delta^-$ ) within these systems where the formation of electron-rich and electron-deficient regions gives a way to modulate the strength and chemical activity of CC bonds. The strength of CC bonds is important within the field of polymer chemistry, where for example, substituent-controlled CC bond cleavage reactions are of interest [14]. For hydrocarbons substitution effects are observed as stabilising electron delocalisations (i.e. charge transfers) [15–17] and are classified as electron-withdrawing/donating inductive effects (i.e. transmitted through bond or through space) [18–21], mesomeric effects (i.e. resonance effects) [20,22–24], electrometric effects (i.e. the temporary displacement of  $\pi$  electrons resulting from reagent attack) [6,25], charge-shift bonding (i.e. refers to the stabilising resonance interaction between the covalent and ionic structures of a bond) [26], and hyperconjugation effects (e.g. negative, positive, and neutral) [25,27–30]. Previously, the effect of substitution on carbon–carbon bond properties have been evaluated in terms of bond length [15,31–33], atomic radii [31,34], bond angle [15,32,35], torsional angle (dihedral angle) [32], bond path angle [35], rotational constants [36], relative bond energy (e.g. bond dissociation energy) [33,37–42], ionisation energy [43,44], strain energy [45,46], resonance energy (RE) of covalent and ionic contribution [26,47], rotational energy barrier [15,48], enthalpy of formation [49], enthalpy of hydrogenation [50,51], heats of combustion [41,51], electronic chemical potential [52], rehybridisation [53–55], chemical hardness [52,56,57], chemical reactivity [57], acidities [58], NMR chemical shift [59], inductive/polar substituent constant [60,61], charge-shift bond character [26,47], distribution of atomic charge and electronic density population at a bond critical point (BCP) [34,62], charge density difference [29,37,45], dipole moment [15,18,52,63], bond order [38], coupling constant [64], and vibrational frequency [42,65]. As well, the following have been used to describe substituent effects on hydrocarbon bonds: bent-bonds (i.e. banana bonds) [66], gauche effects [35], coulombic interactions [29], van der Waals repulsions [67], steric repulsions between H atoms [68], and lone pair  $\pi$ -back bonding [69].

Despite the many investigations conducted on substituted hydrocarbon systems, there has been no quantitative assessment involving a reliable bond strength parameter to evaluate the effect substituents have on the intrinsic bond strength of carbon–carbon bonds. Bond dissociation energy (BDE) is used to quantify the strength of chemical bonds because it is interpreted as a measure of

bond energy. Cremer and co-workers demonstrated that the BDE is inadequate for determining molecular intrinsic bond strengths in cases beyond diatomic molecules because the stabilisation energy includes the electronic reorganisation and geometrical relaxation of the fragments [70]. In addition to BDE, vibrational frequencies [71], bond (electron) density [69,72], and bond length [34,73] have been shown to be inadequate descriptors of bond strength. Moreover, previous work showed a good correlation between CC bond lengths and electron densities at the bond critical point (BCP) for ethane and derivatives [74,75]; but for substituted systems of acetylene and ethylene, a poor correlation was analysed [34]. The local mode force constant  $k^a$ , obtained through the local vibrational mode analysis (defined as LVMA below) originally introduced by Konkoli and Cremer [71,76–78], effectively probes the intrinsic strength of a bond/weak interaction [79] as this quantitative measure does not require bonds/interactions to be dissociated which allows the geometry and electronic structure of a bond to be preserved. The local mode force constant  $k^a$  has been successfully used to systematically investigate the strength of single and multiple covalent bonds of the following:  $C_2$  [80], mono-substituted benzenes [81], carbon-halogen bonds [82,83], and ultra-long C–C bonds [84,85].

Quantitative descriptions for the CC bonds of substituted hydrocarbon systems are important for understanding how substituent effects weaken or strengthen the CC bonds. In this work, we applied LVMA to obtain adequate descriptors of intrinsic bond strength for the  $C\equiv C$ ,  $C=C$ , and  $C-C$  bonds of 36 hydrocarbon derivatives and their parent compounds as well as a conjugated hydrocarbon system as shown in Figure 1. The goals of this work are: (i) to quantitatively assess the intrinsic bond strengths of  $C\equiv C$ ,  $C=C$ , and  $C-C$  bonds for substituted hydrocarbons, (ii) to determine to what magnitude does substitution modulate the intrinsic strengths of  $C\equiv C$ ,  $C=C$ , and  $C-C$  bonds, (iii) to provide a deeper understanding as to how the selected substituents result in weaker or stronger  $C\equiv C$ ,  $C=C$ , and  $C-C$  intrinsic bond strengths.

## 2. Methodology

To analyse the effects of substituents on  $C\equiv C$ ,  $C=C$ , and  $C-C$  intrinsic bond strengths, the equilibrium geometries and vibrational frequencies for a subset of substituted hydrocarbon complexes, involving  $CF_3$ ,  $CH_3$ ,  $CHO$ ,  $F$ ,  $NH_2$ , or  $OH$  groups, their parent compounds, and a conjugated system (Figure 1) were obtained using frozen core coupled-cluster theory with singles, doubles, and perturbative triples (CCSD(T)) [86] in combination with Dunning's cc-pVTZ basis set of triple- $\zeta$  quality

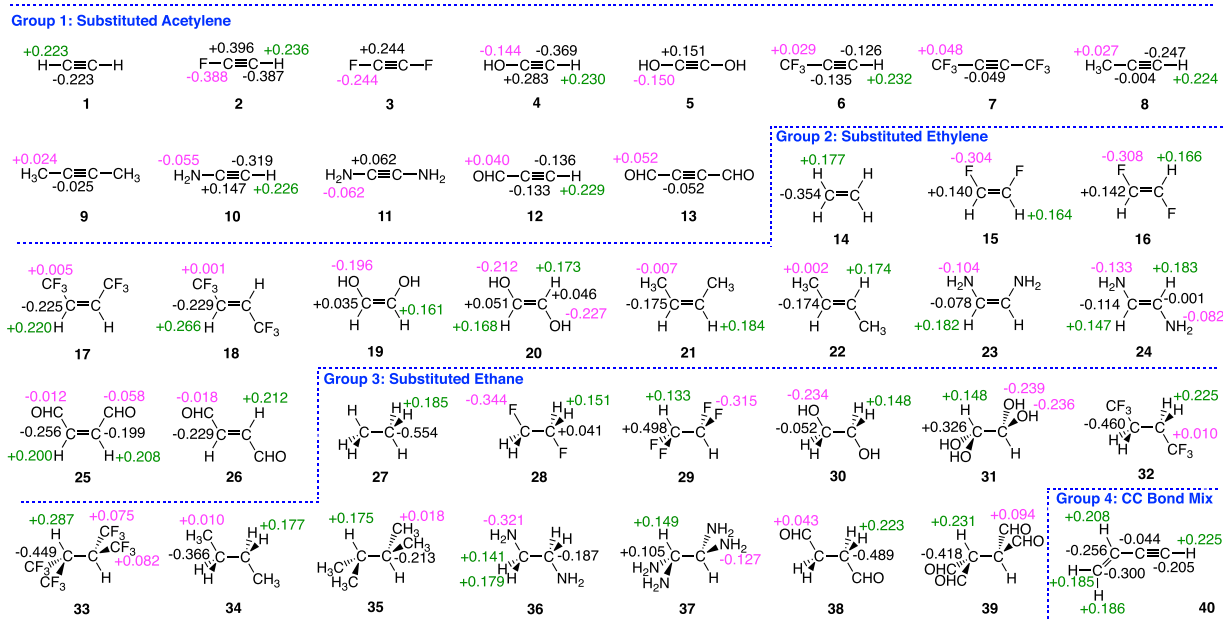


**Figure 1.** A summary of the natural bond orbital charges (NBO) for the atoms/functional groups of systems 1–40. The CCSD(T)/cc-pVTZ level of theory was used for systems 1–32 and 34–40 while CCSD(T)/cc-pVDZ was used for system 33. The NBO charges for C atoms are shown in black, H atoms in green, and corresponding substituent groups in pink.

[87–89]. It is noted that the CCSD(T)/cc-pVDZ level of theory was used for 33 due to the size of the system (eighteen heavy atoms are present). All CCSD(T) calculations were carried out using a convergence criterion of  $10^{-9}$  for self-consistent field iterations and CC amplitudes and a criterion of  $10^{-7}$  hartree/bohr was used for geometry iterations and forces. In most cases, the coupled cluster calculations were performed with the CFOUR program version 2.00 [90,91], although some calculations utilised a local development version with an improved integral transformation step. For all systems, CCSD(T) frequency calculations were performed via analytical second CCSD(T) derivatives [92,93] with the exception of systems 22, 26, 31, 32, 33, 35, and 37 for which finite difference procedures were used. After geometry optimisations, local vibrational mode analysis (LVMA) was used to derive quantitative (intrinsic) bond strength descriptors for all CC bond types using the LModeA software package [79,94]. Because LVMA has been thoroughly explained in Reference [79], only the heart of LVMA is presented below.

Vibrational normal modes provide comprehensive descriptions about bonding interactions and electronic structure of molecules. Normal vibrational modes of polyatomic systems are prone to electronic coupling and mass coupling, the coupling results in delocalised molecular motions (bond stretching/angle bending) where, along with the bond of interest, the motions of additional atoms and/or bonds within the system are considered. Thus, because normal vibrational modes are

not restricted to particular bonds, they cannot be immediately used to assess intrinsic bond strength. Regarding Wilson's secular equation of molecular vibration [95], the electronic coupling of the normal vibrational modes is attributed to the off-diagonal elements of the force constant matrix  $\mathbf{F}^q$

$$\mathbf{F}^q \mathbf{D} = \mathbf{G}^{-1} \mathbf{D} \Lambda \quad (1)$$

where  $\mathbf{q}$  denotes internal coordinates. The Wilson mass-matrix is represented by  $\mathbf{G}$ , the eigenvector matrix  $\mathbf{D}$  is comprised of vibrational eigenvectors  $\mathbf{d}_\mu$  ( $\mu = 1, \dots, N_{vib}$ ), and the diagonal matrix  $\Lambda$  consists of vibrational eigenvalues  $\lambda_\mu$  ( $\lambda_\mu = 4\pi^2 c^2 \omega_\mu^2$ ,  $c =$  constant for the speed of light) where  $\omega_\mu$  are the harmonic vibrational frequencies of the normal mode vectors  $\mathbf{d}_\mu$  expressed in  $\text{cm}^{-1}$ .

The solution to Equation (1) involves the diagonalisation of the force constant matrix  $\mathbf{F}^q$  which involves the transformation of Cartesian coordinates to normal coordinates  $\mathbf{Q}$ . The solution yields a diagonal force constant matrix  $\mathbf{K} = \mathbf{F}^Q$

$$\mathbf{K} = \mathbf{F}^Q = \mathbf{D}^\dagger \mathbf{F}^q \mathbf{D} \quad (2)$$

that is given in normal coordinates  $\mathbf{Q}$  and is not subject to electronic coupling (Equation 2). From Equation (2), one can derive harmonic vibrational frequencies. Nonetheless, the kinematic coupling between modes remains. As demonstrated by Konkoli and Cremer, the kinematic (mass) coupling is eliminated by solving mass-decoupled

Euler Lagrange equations and results in local vibrational modes [76,77,96,97]. Unlike normal vibrational modes, the local vibrational modes ( $\mathbf{a}_i$ ) are free of all mode-mode coupling

$$\mathbf{a}_i = \frac{\mathbf{K}^{-1} \mathbf{d}_i^\dagger}{\mathbf{d}_i \mathbf{K}^{-1} \mathbf{d}_i^\dagger} \quad (3)$$

enabling the local modes to be confined to a particular bond. Regarding Equation (3), the local mode vector  $\mathbf{a}_i$  corresponds to the  $i$ -th internal coordinate  $\mathbf{q}_i$  ( $\mathbf{q}_i$  = bond length, bond angle, dihedral angle, or puckering coordinate). Expressing the local vibrational modes  $\mathbf{a}_i$  in internal coordinates  $i$  allows for these modes to be independent from the type of coordinates used to specify the molecular system of interest. Via the Adiabatic Connection Scheme (ACS) of Zou and Cremer [78,97], it was demonstrated that the normal and local vibrational modes are directly related on a one-to-one basis.

To every local mode  $\mathbf{a}_i$  a corresponding local mode force constant  $k_i^a$  and local vibrational frequency  $\omega_i^a$  can be defined via

$$k_i^a = \mathbf{a}_i^\dagger \mathbf{K} \mathbf{a}_i = (\mathbf{d}_i \mathbf{K}^{-1} \mathbf{d}_i^\dagger)^{-1} \quad (4)$$

and

$$(\omega_i^a)^2 = \frac{1}{4\pi^2 c^2} k_i^a G_{i,i}^a \quad (5)$$

where the diagonal element of the Wilson  $\mathbf{G}$  matrix  $G_{i,i}^a$  contains information pertaining to the mass of the local mode  $\mathbf{a}_i$ . Measures of  $k^a$  (i.e.  $k^a = k_i^a$ ) do not rely upon atomic masses and only on changes in electronic structure (e.g. related to changing a substituent). Thus,  $k^a$  captures pure electronic effects and can be directly used to assess the intrinsic strength of molecular bonds and interactions.

A local mode force constant  $k^a$  can be transformed into a measure of bond strength order (BSO) according to the generalised Badger rule derived by Cremer, Kraka, and co-workers [98,99] through the power relationship:

$$\text{BSO } n = a(k^a)^b \quad (6)$$

The  $k^a$  values of two reference compounds of well-known bond orders were used in order to obtain constants  $a$  and  $b$ . It is assumed that where  $k^a$  is zero the BSO  $n$  value is also zero. As reported in the work of Kraka and co-workers [98], different chemical bonds that are composed of atoms of the same period can be related to a single power relationship (see Equation (6)). Thus, we derive the various C $\equiv$ C, C=C, and C–C bond orders using the same force constant–bond order relationship. For C $\equiv$ C, C=C, and C–C bonds C<sub>2</sub>H<sub>4</sub> (**14**) and C<sub>2</sub>H<sub>6</sub> (**27**) were used as reference molecules with BSO  $n$  values of 2.00 and 1.00, respectively. The  $a$  and  $b$  constants

were determined to be 0.277 and 0.890, respectively. To determine the BSO  $n(\text{CC})$  value for **33** the reference molecules, C<sub>2</sub>H<sub>4</sub> and C<sub>2</sub>H<sub>6</sub>, were recomputed at the CCSD(T)/cc-pVDZ level of theory. The  $a$  and  $b$  constants were determined to be 0.233 and 0.968, respectively.

Natural population charges of CCSD(T) were obtained from the natural bond orbital (NBO) analysis [100,101] with the NBO6 program [102]. Using the AIMAll program, electron density  $\rho_c$  and energy density  $H_c$  values at C $\equiv$ C, C=C, and C–C bond critical points  $r_c$  (BCP), from CCSD(T), were determined [103]. The Cremer–Kraka criterion was used to distinguish bond nature of C $\equiv$ C, C=C, and C–C bonds where covalent bonding is represented by negative energy density  $H_c$  values ( $H_c < 0$ ) and electrostatic interactions are denoted by positive energy density  $H_c$  values ( $H_c > 0$ ) [69,72,104].

Charge transfer stabilisation energies ( $\Delta E^{(2)}$ ) derived from second-order perturbation theory require canonical HF orbitals or Kohn–Sham orbital from DFT. The latter has the advantage of accounting for electron correlation effects. Therefore, we utilised  $\omega\text{B97X-D/cc-pVTZ}$ , a reliable functional that is well-known to reproduce CCSD(T) energies and geometries [105], to compute  $\Delta E^{(2)}$  values.

### 3. Results and discussion

In the following, the results of 40 hydrocarbon derivatives and their parent compounds as well as a conjugated hydrocarbon system possessing single, double, and/or triple CC bonds are presented. First, we present the general trends which are observed with respect to the local mode force constant  $k^a$  values of the targeted CC single, double, and triple bonds. Secondly, the nature of all CC bond interactions is discussed with respect to the energy density  $H_c$ . Third, a comprehensive overview about the BSO  $n(\text{CC})$  values, which we derive directly from the local mode force constant  $k^a$  values, is given.

#### 3.1. General trends

The calculated NBO charges of systems **1–40** are shown in Figure 1 where systems are grouped based upon the type of CC bond. Molecules **1–40** are categorised into four groups. Group 1 consists of systems with C $\equiv$ C bonds such as acetylene and its mono-substituted and di-substituted counterparts (**1–13**). The C=C bonds within Group 2 are those of ethylene and cis-/trans- substituted systems (**14–26**). Group 3 pertains to C–C bonds and includes ethane and di-/tetra- substituted systems (**27–39**) and Group 4 represents a conjugated system having C $\equiv$ C, C=C, and C–C bonds (**40**). Group 1



**Table 1.** CC bond distances (R), local mode frequencies ( $\omega^a$ ), local mode force constants ( $k^a$ ), bond strength orders (BSO  $n$ ), electron densities ( $\rho_c$ ), energy densities ( $H_c$ ), and the energy density ratios ( $\frac{H_c}{\rho_c}$ ) for molecules **1–40**, calculated at the CCSD(T)/cc-pVTZ level of theory with the exception of **33** which was computed using CCSD(T)/cc-pVDZ.

#	Molecule, Symmetry	R (Å)	$\omega^a$ ( $\text{cm}^{-1}$ )	$k^a$ ( $\text{mdyn}/\text{Å}$ )	BSO $n$	$\rho_c$ ( $e/\text{Å}^3$ )	$H_c$ ( $\text{h}/\text{Å}^3$ )	$\frac{H_c}{\rho_c}$ ( $\text{h}/e$ )
<b>CC triple bonds</b>								
1	$\text{HC} \equiv \text{CH}$ , $D_{\infty h}$	1.210	2140	16.191	3.307	2.783	−4.631	−1.664
2	$\text{F}-\text{C} \equiv \text{C}-\text{H}$ , $C_{\infty v}$	1.203	2172	16.671	3.394	2.640	−4.558	−1.727
3	$\text{F}-\text{C} \equiv \text{C}-\text{F}$ , $D_{\infty h}$	1.193	2231	17.588	3.560	2.616	−4.453	−1.702
4	$\text{HO}-\text{C} \equiv \text{C}-\text{H}$ , $C_s$	1.208	2149	16.318	3.330	2.658	−4.570	−1.719
5	$\text{HO}-\text{C} \equiv \text{C}-\text{OH}$ , $C_2$	1.203	2156	16.437	3.352	2.628	−4.403	−1.675
6	$\text{F}_3\text{C}-\text{C} \equiv \text{C}-\text{H}$ , $C_{3v}$	1.208	2146	16.287	3.325	2.775	−4.666	−1.681
7	$\text{F}_3\text{C}-\text{C} \equiv \text{C}-\text{CF}_3$ , $D_{3h}$	1.206	2151	16.370	3.340	2.770	−4.701	−1.697
8	$\text{H}_3\text{C}-\text{C} \equiv \text{C}-\text{H}$ , $C_{3v}$	1.211	2133	16.079	3.287	2.754	−4.641	−1.685
9	$\text{H}_3\text{C}-\text{C} \equiv \text{C}-\text{CH}_3$ , $D_{3h}$	1.212	2128	16.006	3.274	2.743	−4.565	−1.664
10	$\text{H}_2\text{N}-\text{C} \equiv \text{C}-\text{H}$ , $C_s$	1.211	2127	15.997	3.272	2.691	−4.603	−1.710
11	$\text{H}_2\text{N}-\text{C} \equiv \text{C}-\text{NH}_2$ , $C_2$	1.212	2114	15.798	3.236	2.656	−4.391	−1.653
12	$\text{OHC}-\text{C} \equiv \text{C}-\text{H}$ , $C_s$	1.213	2114	15.792	3.235	2.769	−4.585	−1.656
13	$\text{OHC}-\text{C} \equiv \text{C}-\text{CHO}$ , $C_2$	1.217	2082	15.319	3.148	2.753	−4.560	−1.657
<b>CC double bonds</b>								
14	$\text{H}_2\text{C}=\text{CH}_2$ , $D_{2h}$	1.337	1613	9.201	2.000	2.379	−3.149	−1.324
15	$\text{F}(\text{H})-\text{C}=\text{C}(\text{H})\text{F}$ ( <i>cis</i> -), $C_{2v}$	1.330	1637	9.467	2.051	2.467	−3.317	−1.344
16	$\text{F}(\text{H})-\text{C}=\text{C}(\text{H})\text{F}$ ( <i>trans</i> -), $C_s$	1.330	1632	9.412	2.041	2.474	−3.333	−1.347
17	$\text{HO}(\text{H})-\text{C}=\text{C}(\text{H})\text{OH}$ ( <i>cis</i> -), $C_1$	1.336	1618	9.252	2.010	2.422	−3.212	−1.326
18	$\text{HO}(\text{H})-\text{C}=\text{C}(\text{H})\text{OH}$ ( <i>trans</i> -), $C_1$	1.342	1459	7.527	1.673	2.394	−3.141	−1.312
19	$\text{F}_3\text{C}(\text{H})-\text{C}=\text{C}(\text{H})\text{CF}_3$ ( <i>cis</i> -), $C_2$	1.335	1614	9.203	2.000	2.378	−3.203	−1.334
20	$\text{F}_3\text{C}(\text{H})-\text{C}=\text{C}(\text{H})\text{CF}_3$ ( <i>trans</i> -), $C_{2h}$	1.331	1629	9.375	2.034	2.402	−3.203	−1.334
21	$\text{H}_3\text{C}(\text{H})-\text{C}=\text{C}(\text{H})\text{CH}_3$ ( <i>cis</i> -), $C_{2v}$	1.341	1591	8.953	1.952	2.375	−3.118	−1.313
22	$\text{H}_3\text{C}(\text{H})-\text{C}=\text{C}(\text{H})\text{CH}_3$ ( <i>trans</i> -), $C_{2h}$	1.339	1601	9.062	1.973	2.380	−3.136	−1.318
23	$\text{H}_2\text{N}(\text{H})-\text{C}=\text{C}(\text{H})\text{NH}_2$ ( <i>cis</i> -), $C_2$	1.341	1594	8.980	1.957	2.382	−3.127	−1.313
24	$\text{H}_2\text{N}(\text{H})-\text{C}=\text{C}(\text{H})\text{NH}_2$ ( <i>trans</i> -), $C_1$	1.340	1589	8.923	1.946	2.391	−3.172	−1.327
25	$\text{OHC}(\text{H})-\text{C}=\text{C}(\text{H})\text{CHO}$ ( <i>cis</i> -), $C_s$	1.350	1548	8.469	1.858	2.334	−3.018	−1.293
26	$\text{OHC}(\text{H})-\text{C}=\text{C}(\text{H})\text{CHO}$ ( <i>trans</i> -), $C_{2h}$	1.344	1562	8.630	1.889	2.366	−3.096	−1.308
<b>CC single bonds</b>								
27	$\text{H}_3\text{C}-\text{CH}_3$ , $D_{3d}$	1.529	1093	4.223	1.000	1.651	−1.489	−0.902
28	$\text{F}(\text{H})_2-\text{C}-\text{C}(\text{H})_2\text{F}$ , $C_{2h}$	1.516	1119	4.429	1.043	1.816	−1.728	−0.951
29	$(\text{F})_2(\text{H})-\text{C}-\text{C}(\text{H})\text{F}$ , $C_{2h}$	1.522	1120	4.433	1.044	1.899	−1.819	−0.958
30	$(\text{HO})(\text{H})_2-\text{C}-\text{C}(\text{H})\text{OH}$ , $C_{2h}$	1.515	1128	4.496	1.057	1.796	−1.704	−0.949
31	$(\text{HO})_2(\text{H})-\text{C}-\text{C}(\text{H})\text{OH}$ , $C_2$	1.539	1054	3.926	0.937	1.788	−1.629	−0.911
32	$\text{F}_3\text{C}(\text{H})_2-\text{C}-\text{C}(\text{H})_2\text{CF}_3$ , $C_{2h}$	1.526	1093	4.223	1.000	1.668	−1.512	−0.906
33	$(\text{F}_3\text{C})_2(\text{H})-\text{C}-\text{C}(\text{H})\text{CF}_3$ , $C_2$	1.552	1052	3.910	0.871	1.544	−1.205	−0.781
34	$\text{H}_3\text{C}(\text{H})_2-\text{C}-\text{C}(\text{H})_2\text{CH}_3$ , $C_{2h}$	1.529	1081	4.129	0.980	1.678	−1.518	−0.905
35	$(\text{H}_3\text{C})_2(\text{H})-\text{C}-\text{C}(\text{H})\text{CH}_3$ , $C_{2h}$	1.542	1043	3.843	0.919	1.650	−1.448	−0.878
36	$\text{H}_2\text{N}(\text{H})_2-\text{C}-\text{C}(\text{H})_2\text{NH}_2$ , $C_{2h}$	1.522	1100	4.280	1.012	1.742	−1.616	−0.927
37	$(\text{H}_2\text{N})_2(\text{H})-\text{C}-\text{C}(\text{H})\text{NH}_2$ , $C_i$	1.533	1074	4.075	0.969	1.754	−1.599	−0.912
38	$\text{OHC}(\text{H})_2-\text{C}-\text{C}(\text{H})_2\text{CHO}$ , $C_{2h}$	1.519	1105	4.313	1.019	1.694	−1.559	−0.920
39	$(\text{OHC})_2(\text{H})-\text{C}-\text{C}(\text{H})\text{CHO}$ , $C_{2h}$	1.557	957	3.237	0.789	1.521	−1.273	−0.837
<b>CC bond mix</b>								
40	$\text{H}_2\text{C}=\text{C}(\text{H})\text{C}\#C-\text{H}$ , $C_s$							
	triple bond	1.214	2111	15.761	3.229	2.751	−4.604	−1.674
	double bond	1.344	1580	8.824	1.927	2.353	−3.083	−1.310
	single bond	1.434	1266	5.662	1.298	1.949	−2.189	−1.123

is organised by beginning with the parent compound (acetylene) and alternating between mono-substitution and di-substitution starting from the substituent which has the greatest strengthening effect on the  $\text{C} \equiv \text{C}$  bond to the substituent which has the least effect on the  $\text{C} \equiv \text{C}$  bond. For Group 2, after ethylene, only substitutions in *cis*- and *trans*-configurations were considered, the systems were organised by a substituent as done in Group 1. In Group 3, we begin with ethane and proceed to only di-substituted and tetra-substituted systems, where the systems were organised by substituent as done in Groups 1 and 2. Table 1 summarises CC bond distances, local mode frequencies  $\omega^a$ , local mode force constants  $k^a$ ,

bond strength orders BSO  $n$ , electron densities  $\rho_c$ , energy densities  $H_c$ , and their ratios  $\frac{H_c}{\rho_c}$  for systems **1–40**. The data of Table 1 are organised in the same manner as that done within Figure 1; note that for the conjugated system of Group 4 the data is presented starting from the  $\text{C} \equiv \text{C}$  bond ending with the  $\text{C}-\text{C}$  bond.

Figure 2 shows the correlation between the bond strength order BSO  $n(\text{CC})$  and the CC local mode force constant  $k^a$  (Figure 2). The color scheme of Figure 2 is as follows: red data points represent Group I systems, green data points represent Group 2 systems, and blue data points denote Group 3 systems. The circular data points within Figure 2 represent the parent systems (**1**, **14**, **27**).

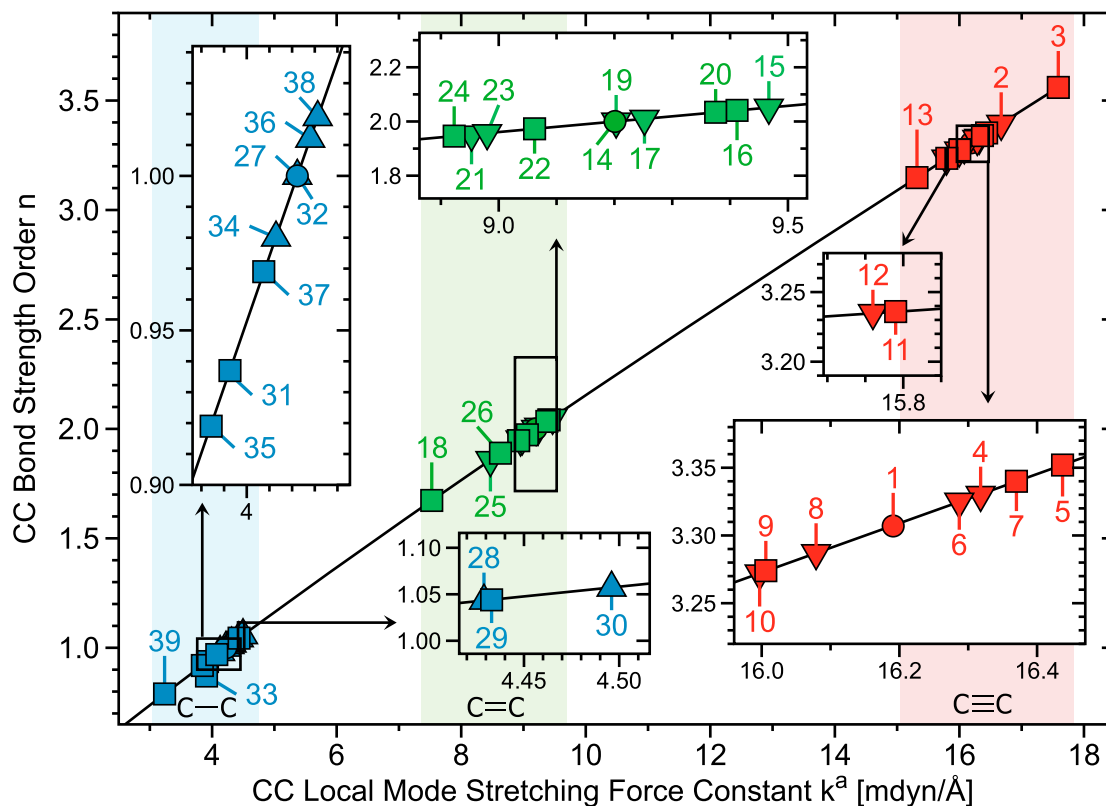


**Figure 2.** Bond strength order (BSO)  $n$  values of **1–39** calculated from  $k^a$  via Equation (6). The CCSD(T)/cc-pVTZ level of theory was used for systems **1–32** and **34–39** and CCSD(T)/cc-pVDZ was used for system **33**. The red points denote Group 1 systems, the green points indicate Group 2 molecules, and the blue points represent systems of Group 3.

The triangle data points represent the mono-, cis-, and di-substitutions of  $C_2H_2$ ,  $C_2H_4$ , and  $C_2H_6$ . The square data points represent the di-, trans-, and tertrial-substitutions of  $C_2H_2$ ,  $C_2H_4$ , and  $C_2H_6$ .

Figure 3 shows the relationship between the CC local mode force constant  $k^a$  and the corresponding CC bond lengths of molecules **1–39**. It is noted that the computed CC bond lengths for all parent systems (see Table 1) are in agreement with their experimental counterparts [106–108]. In general, it is widely believed that a longer bond distance equals a weaker bond. However, as mentioned earlier, previous publications involving various bonding scenarios have demonstrated that this is not always the case [70,73,85,109–111]. As shown in Figure 3, there exists an inverse exponential correlation between bond strength and bond length ( $R^2 = 0.992$ ). In this present study, a large deviation from this relationship is observed only for molecule **18** which was found to be weaker than other double bonds of similar length.

### 3.2. Carbon–Carbon bond nature

How a substituent modulates the CC bonds attributed to acetylene, ethylene, and ethane differs due to the

variation of s-character on carbon. As the s-character on the carbon atoms increases ( $sp^3 < sp^2 < sp$ ) the attractive forces (covalent character) between the electrons and nucleus increase to result in a shorter/stronger CC bond [19,24]. The  $\sigma$  bond is held primarily responsible for the stability of hydrocarbon systems as the overlapping of s-orbitals, in comparison to the  $\pi$ -overlapping of p-orbitals to form  $\pi$  bonds, which allocates electron density above and below the plane of the CC bond, localises the electron density along the plane of the carbon atoms [112].

From Figure 4, we observe the correlation between the local mode force constant  $k^a$  and energy density  $H_c$  (i.e. covalent bond character) to be exceptional ( $R = 0.990$ ); outliers **3**, **5**, **11**, **18**, and **39** demonstrate that the local mode force constant, unlike  $H_c$ , does not reflect the electronic structure at only a single point (i.e. bond critical point,  $r_c$ ) but considers, overall, the electronic environment of atoms and the bond which they constitute [79]. In particular, this trend is very poor for  $C\equiv C$  triple bonds. With regard to **2**, **3**, **4** and **5** the di-substitution causes the energy density at the  $C\equiv C$  BCP ( $H_c$ ) to increase further (covalent character decreases) alongside increasing bond strength (see Table 1 and Figure 4). Such discrepancies can be a result of the fact that for mono-substituted species the polarisation of the CC bond shifts

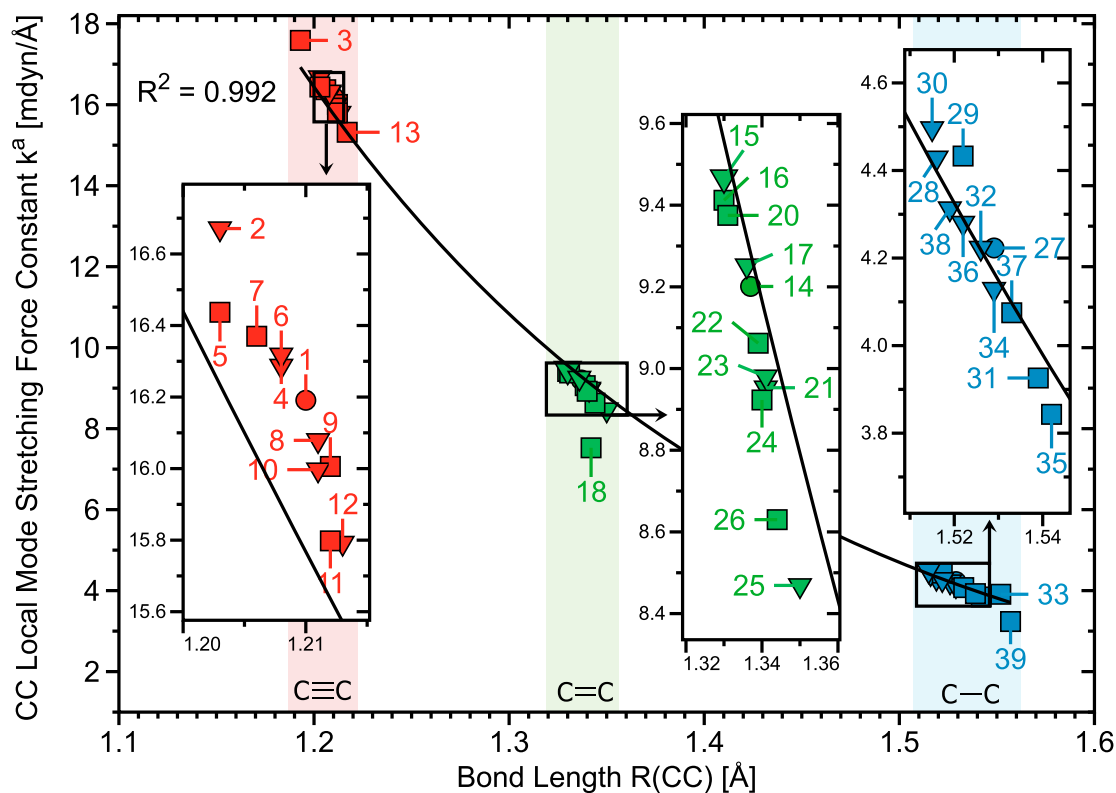


**Figure 3.** The local mode force constant ( $k^a$ ) plotted against the corresponding CC bond lengths belonging to systems 1–39. Bond distance values calculated at the CCSD(T)/cc-pVTZ level of theory for molecules 1–32; 34–39 and that of 33 was computed at the CCSD(T)/cc-pVDZ level of theory. An exponential fit on this relationship yields an  $R^2$  value of 0.992, respectively.

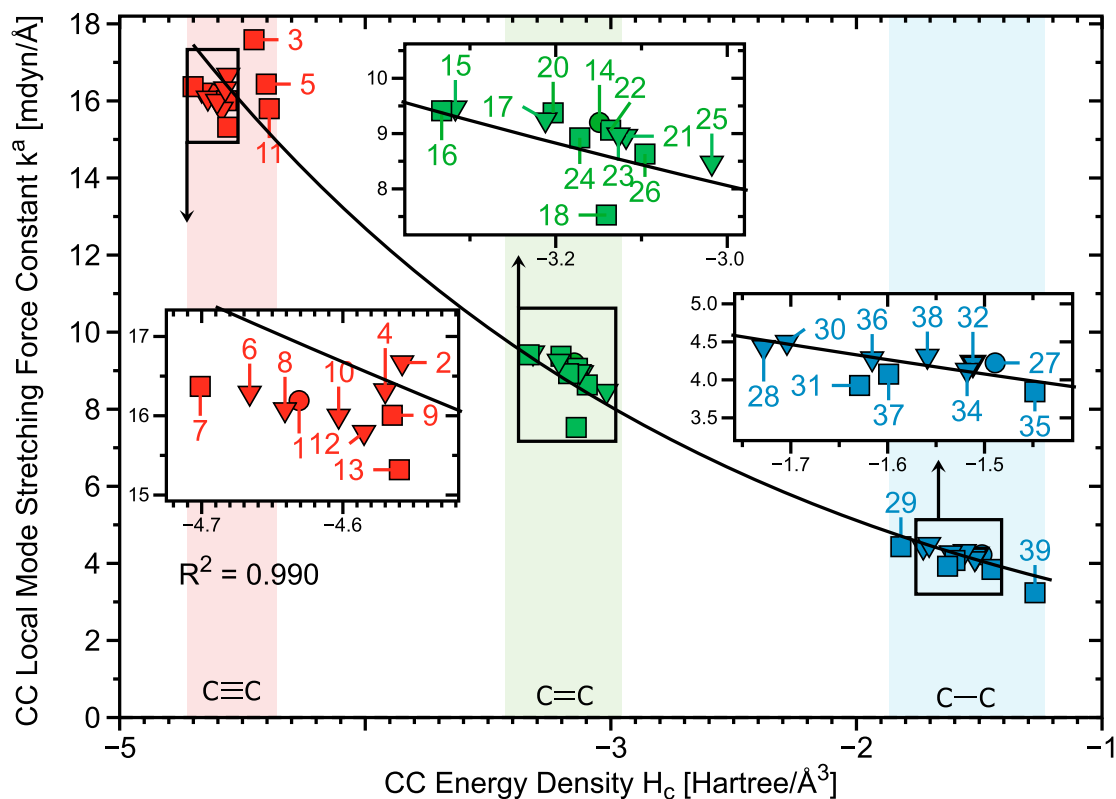


**Figure 4.** The correlation between the local mode force constant ( $k^a$ ) and energy density values  $H_c$  for all systems investigated, for systems 1–32; 34–39 values were calculated at the CCSD(T)/cc-pVTZ level of theory while those of 33 were tabulated using CCSD(T)/cc-pVDZ methodology. An  $R^2$  value of 0.990 resulted from fitting an exponential model to the data.



the BCP away from the centre. As well, in this study, the electron density  $\rho_c$  and energy density  $H_c$  values measure local features which pertain more to the  $\sigma$  bonds than the  $\pi$  bonds. Thus, in the case that an electronegative substituent favours an increase of density within the  $\pi$  region over the  $\sigma$  region one may see the overall electron  $\rho_c$  and energy density  $H_c$  values at the BCP to decrease, even if the density within the  $\pi$  region increases, as  $\rho_c$  and  $H_c$  values reflect the electronic structure at a single point  $r_c$  that pertains more to the  $\sigma$  region. On another note, we do observe a general trend for the C=C and C–C bond strengths where the strength of such CC bonds decreases in parallel with decreasing covalent character.

### 3.3. Bond strength order $n$

As depicted in Figure 2, the C–C bonds of ethane analogs **28–39** show the smallest deviation in bond strength [BSO  $n(\text{C–C})$  values range from 0.789 to 1.057] reflecting the significant change (weak)  $\pi$  orbital interactions have on the CC bond strengths for double bonded [BSO  $n(\text{C=C})$  from 1.673 to 2.051 (**15–26**)] and triple bonded systems [BSO  $n(\text{C}\equiv\text{C})$  from 3.148 to 3.560 (**2–13**)]. Our results are in line with the fact that the modulation of C=C and C $\equiv$ C bonds is more challenging than the modulation of a C–C single bond as the orbital overlaps between  $\sigma$  and  $\pi$  orbitals result in stronger CC bonds.

The difference between the BSO  $n$  of single and double bonds (0.62 BSO  $n$  units) is smaller than that between double and triple bonds (1.10 BSO  $n$  units) validating that the power relationship is in agreement with the universally accepted chemical principle that a higher bond order leads to a higher bond strength. With regard to Group 1, we find that the BSO  $n(\text{C}\equiv\text{C})$  values of derivatives **2–7**, which reflect mono- or di-substitution with  $-\text{CF}_3$ ,  $-\text{F}$ , or  $-\text{OH}$  groups, are larger than that of acetylene **1** where difluoroacetylene (**3**) results in the strongest C $\equiv$ C bond with a BSO  $n$  value of 3.560, respectively. The Group 1 analogs **8–13** reveal that substitution with  $-\text{CH}_3$ ,  $-\text{NH}_2$ , and  $-\text{CHO}$  groups lead to C $\equiv$ C bond weakening, where **13** acquires the weakest C $\equiv$ C bond (BSO  $n = 3.148$ ). Similarly, BSO  $n(\text{C=C})$  values larger than that of **14** (BSO  $n = 2.00$ ) are observed for Group 2 systems with  $-\text{CF}_3$ ,  $-\text{F}$ , or  $-\text{OH}$  substituents (in cis- and trans-configurations) with the exception of trans-1,2-dihydroxyethylene **18** which acquires the weakest C=C bond with a BSO  $n$  value of 1.673. Overall, cis-1,2-difluoroethene **15** is found to acquire the strongest C=C bond (BSO  $n = 2.051$ ). The substituent groups amine, trifluoromethyl, formyl, and methyl are observed to decrease the C–C bond strength order below that of ethane (**27**) when applied to form 1,2-di-substituted and 1,1,2,2-tetra-substituted ethanes (see Table 1), the

1,1,2,2-tetra-substitution of ethane with  $-\text{CHO}$  yields the weakest C–C bond for Group 3 (BSO  $n = 0.789$ ).

## 3.4. Bond modulation properties of specific substituents

### 3.4.1. Fluorination

Though previous literature has noted fluorine to have destabilising effects for acetylene based derivatives [40], we observe the single and double substitution of HCCH with fluorine (**2**, **3**) to yield, in contrast to that of acetylene (**1**), exceptionally strengthened C $\equiv$ C bonds [BSO  $n(\text{C}\equiv\text{C})$ : 3.307 (**1**); 3.394 (**2**); 3.560 (**3**)]. The inductive (i.e.  $-I$ ) effect of fluorine, which occurs via the attraction of  $\sigma$  electrons and repulsion of  $\pi$  electrons [20,46], is reflected in the natural charges of the carbon atoms comprising the C $\equiv$ C bonds of **2** and **3** as these charges increase compared to the parent (**1**) (see Figure 1). Moreover, the electron density at the BCP of C $\equiv$ C decreases as HCCH undergoes substitution with fluorine and the  $\sigma$  orbital undergoes contraction, as reflected from shorter C $\equiv$ C bond lengths (see Table 1). The most impactful charge transfer events on the C $\equiv$ C bond regions within **2** and **3** are observed to involve delocalisation of electrons from the lone pair (lp) of fluorine to the  $\sigma^*$  and  $\pi^*$  orbital of the C $\equiv$ C bond where the overall sum of  $\Delta E^{(2)}$  values, resulting from such instances of hyperconjugation, is greater within **2** in comparison to **3** [ $\Delta E^{(2)} = 85.79$  kcal/mol (**2**), 80.43 kcal/mol (**3**)] and leads to a weaker C $\equiv$ C bond within **2** where the covalent bond character is smaller than that of **3** (see Table 1).

Di-fluorination of ethylene (**14**), in a cis- or trans-configuration (**15** and **16**), causes the C=C bonds to shorten and strengthen [BSO  $n(\text{CC})$ : 2.051 (**15**); 2.041 (**16**)]. The C=C bond of **15**, being stronger than that of **16**, is in agreement with previous findings where di-fluorinated ethylene was found to energetically prefer the cis-conformation [113]. The electron density at the C=C BCP is seen to be larger in **16** and **15** (see Table 1); as the F atoms withdraw electrons away from C=C through the bonds ( $-I$ ), the charges of the C=C atoms increase (see Figure 1). Moreover, from NBO analysis, we observe that the overall charge transfer between lp(F) orbitals and  $\sigma^*$ ,  $\pi^*(\text{C=C})$  orbitals is predominantly influenced by the interaction between lp(F) orbitals and  $\pi^*(\text{C=C})$  orbitals where such an interaction occurs at a greater magnitude within **15**, in contrast to **16** [sum of  $\Delta E^{(2)} = 78.95$  (**15**), 72.89 kcal/mol (**16**)].

Similarly to acetylene and ethylene derivatives, the fluorination of ethane increases the strength of the carbon-carbon single bond [BSO  $n(\text{CC}) = 1.043$  (**28**), 1.044 (**29**)]. From Figure 1, we observe the NBO charges of C–C atoms, in comparison to that of **27**, to increase

alongside the attachment of additional F groups from **28** to **29**. We observe **29** to have a longer C–C bond in contrast to **28** as to counterbalance steric repulsion effects between the four F atoms (see Table 1). The C–C bonds of **28** and **29** are stronger than that of ethane due to greater covalent bond characters [ $H_c = -1.489$  (**27**),  $-1.728$  (**28**),  $-1.819$  h/Å<sup>3</sup> (**29**)], where **29** is stronger than **28** as it acquires a greater covalent bond nature.

### 3.4.2. Hydroxylation

Systems **4** and **5** represent the mono-hydroxylation and di-hydroxylation of acetylene (**1**). The CC bond becomes stronger as OH groups replace H atoms [BSO  $n(\text{C}\equiv\text{C}) = 3.330$  (**4**);  $3.352$  (**5**)]. As the C≡C bond strength becomes stronger the C≡C bond distance becomes shorter (see Table 1). From NBO charges, we see that OH groups have an +I effect on the C≡C bond region (see Figure 1). Moreover, from stabilization energies  $\Delta E^{(2)}$ , a larger amount of charge transfer, from  $\sigma(\text{C}-\text{O})$  and  $\sigma(\text{O}-\text{H})$  orbitals to  $\pi^*(\text{C}\equiv\text{C})$  orbitals occurs within **4** with respect to **5** [sum of  $\Delta E^{(2)} = 23.77$  (**4**),  $22.14$  kcal/mol (**5**)]. Due to a larger amount of electron delocalisation, **4** acquires a less covalent C≡C bond character compared to **5** (see Table 1). In general, the C≡C strengths of **4** and **5** are larger than that of **1** due to an increase of covalent bond nature [ $H_c = -4.631$  (**1**),  $-4.570$  (**4**),  $-4.403$  h/Å<sup>3</sup> (**5**)].

Di-hydroxylation of C<sub>2</sub>H<sub>4</sub> strengthens the C=C bond when substitution follows a cis-configuration (**17**) and weakens the C=C bond when following a trans-configuration (**18**) [BSO  $n(\text{CC}) = 2.010$  (**17**);  $1.889$  (**18**)]. As the natural charges of the C atoms comprising the C=C become electropositive from **17** to **18** the C=C bond distance becomes longer (see Figure 1 and Table 1). Additionally, NBO analysis reveals that the C=C bond region of **18** faces a larger extent of charge transfer between  $\sigma(\text{O}-\text{H})$  and  $\pi^*(\text{C}=\text{C})$  orbitals in comparison to **17** [sum of  $\Delta E^{(2)} = 4.15$  (**17**),  $9.32$  kcal/mol (**18**)]. A greater extent of hyperconjugation effects pertaining to the carbon–carbon double bond region of **18** yields a less covalent C=C bond and in turn a weaker C=C bond in comparison to **17** [ $H_c = -3.212$  (**17**),  $-3.141$  h/Å<sup>3</sup> (**18**)].

Substitution of ethane (**27**) with OH strengthens the C–C bond via di-hydroxylation (**30**) and weakens C–C bond strength through tetra-hydroxylation (**31**) [BSO  $n(\text{CC}) = 1.057$  (**30**);  $0.937$  (**31**)]. The changes in bond strength correlate with changes of C–C bond length, where as the C–C bond becomes stronger the bond length becomes shorter and vice versa [R(CC):  $1.529$  (**27**),  $1.515$  (**30**),  $1.539$  Å (**31**)]. As the hydroxylation of ethane proceeds, the charge transfer events between  $\sigma(\text{C}-\text{C})$  and  $\sigma^*(\text{O}-\text{H})$  become slightly larger [sum of

$\Delta E^{(2)} = 3.66$  (**30**),  $4.38$  kcal/mol (**31**)]. The strengthening of the CC bond within **30** is in line with increasing covalent bond character observed via the  $H_c$  value increasing from  $-1.489$  to  $-1.704$  h/Å<sup>3</sup>. The weakening of the C–C bond within **31**, in contrast to **30**, is due to a smaller covalent C–C bond nature within **31** ( $H_c = -1.629$  h/Å<sup>3</sup>).

### 3.4.3. Trifluoromethylation

Upon mono-trifluoromethyl substitution of acetylene (**6**), the NBO charges of the carbon–carbon atoms comprising the C≡C bond decrease (see Figure 1 and Table 1). The  $\sigma$ -withdrawing character of CF<sub>3</sub> [21,46], attributed to the inductive through bond  $\sigma$  withdrawing (–I) effect of fluorine [46], polarises the C≡C bonds leading to a delocalisation of the  $\sigma$  bond, a loss of electron density  $\rho_c$  at the C≡C BCP (see Table 1), and a flattening and contraction of the  $\sigma$  orbital. The contraction of the C≡C sigma orbital increases the  $\pi$  orbital overlap as revealed from the strengthening and shortening of the CC triple bond within mono-trifluoromethylacetylene **6**, with respect to that of the parent compound (**1**). The C≡C atoms within di-trifluoromethylacetylene (**7**), in comparison to those of **6**, are separated at a shorter distance and have smaller NBO charges (see Table 1). The NBO charges of C≡C atoms for **7** are smaller than those of **6** due to CF<sub>3</sub> substituents being present on both ends where two dipole moments, which delocalise electrons from the C≡C region towards the trifluoromethyl groups, cause the overall electron density at the C≡C BCP to decrease further (see Figure 1 and Table 1). This additional decrease in the electron density  $\rho_c$  at the C≡C BCP within **7** causes the  $\sigma$  orbital of the carbon–carbon triple bond to contract further than that occurring within **6**, thus, the extent of  $\pi$  orbital overlap within the C≡C region of **7** increases as reflected from the shorter C≡C bond distance [R(CC) =  $1.208$  (**6**),  $1.206$  Å (**7**)] and the corresponding BSO  $n$  values [ $3.325$  (**6**),  $3.340$  (**7**)]. From the stabilisation energy values, relevant to the charge transfer events between  $\sigma$ ,  $\pi(\text{C}\equiv\text{C})$  and  $\sigma^*(\text{C}-\text{CF}_3)$  orbitals, we observe that less positive and negative hyperconjugation takes place between  $\sigma$ ,  $\pi(\text{C}\equiv\text{C})$  and  $\sigma^*(\text{C}-\text{CF}_3)$  orbitals within system **7** [sum of  $\Delta E^{(2)} = 10.50$  kcal/mol (**6**),  $6.01$  (**7**)]. As hyperconjugation effects are more extensive within **6**, di(trifluoromethyl)substituted acetylene (**7**) has a shorter and stronger C≡C bond due to a greater covalent bond character [ $H_c = -4.67$  (**6**),  $-4.70$  h/Å<sup>3</sup> (**7**)].

The cis- and trans-trifluoromethylation of ethylene (**19** and **20**) modulates C=C bond strength in a similar manner to the modulation of the C≡C bond via mono- and di-trifluoromethyl substitution of acetylene

(6 and 7) (see Table 1). The steric repulsion between the large CF<sub>3</sub> groups of cis-1,2-difluoromethylethylene (19) yield a longer C=C distance with respect to trans-1,2-difluoromethylethylene (20). As seen from C=C NBO charges (see Figure 1), the intramolecular dipole moments of the C-CF<sub>3</sub> bond interactions within 19 are greater than that of 20 where the electron density  $\rho_c$  value at the C=C BCP is greater within 20 in comparison to 19 (see Table 1). The C=C bond within 20 is shorter and stronger than that of 19 as a result of a higher covalent nature (see corresponding  $H_c$  values in Table 1) due to a lesser extent of charge transfer events (i.e. hyperconjugation) occurring between  $\sigma$ ,  $\pi$ (C=C) and  $\sigma^*$ (C-CF<sub>3</sub>) within system 20 with respect to 19 [sum of  $\Delta E^{(2)}$  = 6.12 (19), 4.96 kcal/mol (20)].

The strength of the C-C bond within 1,2-difluoromethylethane (32) is similar to that of ethane (27) and is stronger than that of 1,1,2,2-tetratetrafluoromethylethane (33) (see Table 1). The -I effect of CF<sub>3</sub> initiates charge transfer between  $\sigma$ (C-C) and  $\sigma^*$ (C-F) where greater stabilisation energy values result for 33 in comparison to 32 [sum of  $\Delta E^{(2)}$  = 6.96 (32), 8.68 kcal/mol (33)], the smaller amount of hyperconjugation within 32 results in a C-C bond that acquires a greater covalent character [ $H_c$  = -1.512 (6), -1.205 h/Å<sup>3</sup> (7)]. As well, the electron density  $\rho_c$  at the C-C BCP is greater for 32 in contrast to 33 (see Table 1). These results reveal that the C-C bond within system 1,1,2,2-tetratetrafluoromethylethane (33) is weaker and longer than that of 1,2-difluoromethylethane (32) due to a greater extent of steric repulsion and positive hyperconjugation where such interactions lead to a decrease of the covalent character within the C-C bond region.

### 3.4.4. Methylation

Mono-methylation of acetylene (8) causes C≡C bond elongation and weakening [BSO  $n$ (CC) = 3.307 (1); 3.287 (8)]. The  $\sigma$ -donating character of CH<sub>3</sub> occurs through the bond by means of an (electron pushing) +I effect [18,46,62,63]. In general, the +I effect pushes electron density away from the  $\alpha$ -carbon (the site of substituent attachment) towards the neighbouring carbon atom (i.e.  $\beta$ -carbon), this type of bond polarisation is reflected from the C≡C NBO charges of 8 (see Figure 1). The polarisation occurring along the C≡C bond region within 8 causes the electron density  $\rho_c$  at the C≡C BCP to decrease in contrast to the parent system (see Table 1). Because such a redistribution of C≡C electron density, caused by the use of CH<sub>3</sub> substituents, has been noted to primarily effect the  $\pi$  bonds [18,48,63], the elongation of the C≡C bond which occurs from the mono-methylation of acetylene (8), are fundamentally attributed to the  $\pi$ -bonding region [51].

The di-methylation of acetylene (9) yields a weaker C≡C bond in contrast to 8 [BSO  $n$ (CC) = 3.274 (9)]. The  $\Delta E^{(2)}$  values, which are relevant to the charge transfer events from  $\sigma$ (C-H) →  $\sigma^*$ (C≡C) and  $\sigma$ (H<sub>3</sub>C-C) →  $\sigma^*$ (C≡C) (where C-H bonds pertain to that of CH<sub>3</sub>), are greater for 9 in comparison to 8 [sum of  $\Delta E^{(2)}$  = 21.50 (8), 39.88 kcal/mol (9)]. Thus, di-methylacetylene (9) acquires a weaker C≡C bond in contrast to mono-methylacetylene (8) due to a larger magnitude of positive hyperconjugation (i.e.  $\sigma$  withdrawal) on the C≡C bond region. The smaller hyperconjugation effects within 8, in contrast to 9, lead to 8 acquiring a larger electron density  $\rho_c$  at the C≡C BCP which, in turn, establishes a stronger and shorter C≡C bond for mono-methylacetylene (8) in comparison to di-methylacetylene (9) (see Table 1).

Similarly to the acetylene analogs (8 and 9), both cis-1,2-di-methylethylene (8) and trans-1,2-methylethylene (9) lengthen and weaken the C=C bond [BSO  $n$ (CC) = 1.952 (21), 1.973 (22)]. The longer C=C bond distance of 21, with respect to 22, reveals that a greater extent of steric hindrance between the methyl substituents of cis-2-butene is present (21). The  $\Delta E^{(2)}$  value, stemming from similar instances of positive hyperconjugation seen on the C≡C bond of mono- and di-methylacetylene, is greater for 21 in comparison to 22 [sum of  $\Delta E^{(2)}$  = 15.18 (21), 14.18 kcal/mol (22)]. Overall, the greater extent of positive hyperconjugation within 21, with respect to its trans-counterpart 22, causes the covalent C=C character for 21 to be smaller than that of 22 [ $H_c$  = -3.118 (21), -3.136 h/Å<sup>3</sup> (22)] resulting in 22 attaining a much weaker C=C bond in contrast to 21.

Di- and tetra-methylation of ethane causes the C-C bond strength to decrease [BSO  $n$ (CC) = 0.980 (34), 0.919 (35)]. NBO analysis reveals that a greater extent of C-C bond polarisation taking place within 35 results in smaller carbon-carbon NBO charges in contrast to those of 34 (see Figure 1) and the C-C electron density  $\rho_c$  at the C-C BCP is smaller for 35 with respect to 34 (see Table 1). A lower electron density  $\rho_c$  is found at the BCP of the C-C of 35 due to a greater magnitude of positive hyperconjugation occurring between methyl  $\sigma$ (C-H) and  $\sigma^*$ (C-C) orbitals of 1,1,2,2-tetramethylethane (35) with respect to that of butane (34) [ $\Delta E^{(2)}$  = 8.10 (34), 17.76 kcal/mol (35)]. Because the C-C bond of 35 is exposed to a greater extent of hyperconjugation effects the CC single bond is less covalent, and in turn, weaker than that of 34 [ $H_c$  = -1.518 (34), -1.448 h/Å<sup>3</sup> (35)].

### 3.4.5. Amination

Single and double amination of acetylene 1 causes C≡C bond strength to decrease [BSO  $n$ (C≡C) = 3.272 (10); 3.236 (11)] along with slight increases in the C≡C bond length (see Table 1). The electron-pushing inductive (+I)

nature of  $\text{NH}_2$  is reflected from the charges of carbon atoms involved in  $\text{C}\equiv\text{C}$  bonding. For **10**, the  $\alpha$ -carbon atom (carbon atom at site of substituent attachment) decreases drastically in charge ( $\alpha$ -C charge: +0.147 e) alongside the increase of  $\beta$ -carbon atom charge ( $\beta$ -C charge: -0.319 e), the charge at the  $\beta$ -carbon atom increases by 0.146 e in comparison to that of **1** (see Figure 1). Further, the weaker  $\text{C}\equiv\text{C}$  bonds of **11**, with regard to **10**, are attributed to a decrease in covalent character where the covalent bond character of **11** is smaller than that of **10**. From the electron density analysis of the  $\text{C}\equiv\text{C}$  bonds for **10** and **11**, it is apparent that the +I effect of amine is enhanced by additional substitution due to the polarisation of electron density at the  $\text{C}\equiv\text{C}$  BCP, where  $\rho_c$  and covalent bond character continually decrease as the amination of  $\text{C}\equiv\text{C}$  proceeds (see Table 1). Because  $\text{NH}_2$  has been classified as a  $\pi$  donor and  $\sigma$  acceptor the charge transfer events between  $\sigma(\text{C}\equiv\text{C}) \rightarrow \sigma^*(\text{N}-\text{H})$ ,  $\sigma(\text{N}-\text{H}) \rightarrow \pi^*(\text{C}\equiv\text{C})$  and  $\text{lp}(\text{N}) \rightarrow \pi^*(\text{C}\equiv\text{C})$  for **10** and **11** are considered. The total stabilisation energy [i.e.  $\Delta E^{(2)}$ ] affiliated with electron donation from  $\sigma$ ,  $\pi(\text{C}\equiv\text{C})$  to  $\text{NH}_2$  is 13.73 kcal/mol for **10** and 22.3 kcal/mol for **11**; the overall charge transfer from  $\text{NH}_2$  to  $\sigma^*$ ,  $\pi^*(\text{C}\equiv\text{C})$  yields stabilisation energy  $\Delta E^{(2)}$  values of 73.69 kcal/mol and 142.84 kcal/mol for systems **10** and **11**, respectively. From these  $\Delta E^{(2)}$  values, it is evident that as amine is substituted onto the  $\text{C}\equiv\text{C}$ , the  $\sigma$  withdrawing and  $\pi$  donating nature of amine amplifies in parallel to diminishing covalent  $\text{C}\equiv\text{C}$  bond character; which results in a weaker  $\text{C}\equiv\text{C}$  bond strength for **11** with respect to **10** due to a greater extent of electron delocalisation primarily towards  $\pi^*(\text{C}\equiv\text{C})$  orbitals.

Substitution of ethylene with  $\text{NH}_2$  groups to produce cis- and trans-configurations (**23** and **24**) causes the  $\text{C}=\text{C}$  bond to become weaker [BSO( $\text{C}=\text{C}$ )  $n = 1.957$  (**23**); 1.946 (**24**)]. In contrast to **23**, it is observed that the  $\text{C}=\text{C}$  bond region of **24** involves a greater magnitude of charge transfer events, where the overall charge transfer to  $\pi^*(\text{C}=\text{C})$ , for **23** and **24**, results in stabilisation energy  $\Delta E^{(2)}$  values of 67.10 kcal/mol and 48.80 kcal/mol, respectively. Due to a smaller extent of electron delocalisation primarily towards  $\pi^*(\text{C}=\text{C})$  orbitals, **24** acquires a larger covalent bond character and in turn a stronger  $\text{C}=\text{C}$  bond with respect to **23** (see Table 1).

Amination of ethane strengthens the  $\text{C}-\text{C}$  bond via di-amination (**36**) and weakens the  $\text{C}-\text{C}$  bond through tetra-amination (**37**) [BSO  $n(\text{CC})$ : 1.012 (**36**); 0.969 (**37**)]. Accordingly, the  $\text{C}-\text{C}$  bond length of **36** decreases while the bond length of **37** increases compared to **27** [ $R(\text{CC}) = 1.529$  (**27**), 1.522 (**36**); 1.533 Å (**37**)]. The stronger and shorter  $\text{C}-\text{C}$  bond length for **36** corresponds to a larger covalent  $\text{C}-\text{C}$  bond nature for **36** with regard to **37** [ $H_c = -1.616$  (**36**),  $-1.599$  h/Å<sup>3</sup> (**37**)]

where the smaller covalent  $\text{C}-\text{C}$  bond nature of **37** is attributed to a greater amount of electron delocalisation between  $\sigma(\text{C}-\text{C})$  and  $\sigma^*(\text{N}-\text{H})$  [sum of  $\Delta E^{(2)} = 4.40$  (**36**), 9.44 kcal/mol (**37**)].

### 3.4.6. Formylation

Mono and di-formylation of **1** elongates and weakens the  $\text{C}\equiv\text{C}$  bond (see **12** and **13** within Table 1). The NBO charges of systems **12** and **13** reflect the -I (through-bond) effect of CHO on the  $\text{C}\equiv\text{C}$  bond region; for example, with regard to **12**, the charge of the carbon atom, which is adjacent to the carbon atom at which the substituent is attached, decreases drastically in comparison to that of the parent (**1**) (see Figure 1). Moreover, the withdrawing effect (-I) of CHO causes the electron density to diminish as the  $\text{C}\equiv\text{C}$  bond undergoes additional substitution (see Table 1). Charge transfer occurring from  $\sigma(\text{C}\equiv\text{C}) \rightarrow \sigma^*(\text{OHC}-\text{C})$  reveal that the  $\text{C}\equiv\text{C}$  of **13** is weaker than that for **12** due to a larger amount of electron delocalisation [sum of  $\Delta E^{(2)} = 5.77$  (**12**); 10.10 kcal/mol (**13**)]. Because **13** acquires a greater  $\Delta E^{(2)}$  the covalent nature, and in turn strength, of the  $\text{C}\equiv\text{C}$  bond declines as the formylation of **1** proceeds [ $H_c = -4.631$  (**1**),  $-4.585$  (**12**),  $-4.560$  (**13**)]. As mentioned in section 3.3, the weakest  $\text{C}\equiv\text{C}$  bond within Group 1 results from the di-formylation of acetylene (**13**).

Formyl substitution of **14**, in the form of cis- (**25**) and trans-configurations (**26**), leads to a weakening of the  $\text{C}=\text{C}$  bond [BSO  $n(\text{CC})$ : 1.858 (**25**); 1.889 (**26**)] in a similar manner to the  $\text{C}\equiv\text{C}$  bond weakening seen for formylated acetylene (**12** and **13**). The  $\text{C}=\text{C}$  bond of **25** is weaker and longer than that of **26** (see Table 1). Via electron density analysis we find the electron density at the  $\text{C}=\text{C}$  BCP to decrease further when formyl groups are in a cis-conformation (see Table 1). Moreover, we observe **25** to acquire a longer  $\text{C}=\text{C}$  bond than that of **26** as a greater extent of steric repulsion occurs between the CHO substituents of cis-1,2-formylethylene (**25**); the steric repulsive forces within **25** leads to a smaller covalent  $\text{C}=\text{C}$  bond character in comparison to **26** which causes a weakening of the  $\text{C}=\text{C}$  bond (see Table 1).

Formylation of ethane (**27**) results in shorter and longer bonds as the substitution proceeds [BSO  $n(\text{CC})$ : 1.019 (**38**); 0.789 (**39**)]. The  $\text{C}-\text{C}$  bonding region of **38** involves charge transfer events from  $\sigma(\text{C}-\text{C})$  to formyl  $\sigma^*(\text{C}-\text{H})$  orbitals, where the sum of  $\Delta E^{(2)}$  for the electron delocalisation between  $\sigma(\text{C}-\text{C})$  and  $\sigma^*(\text{C}-\text{H})$  is 4.38 kcal/mol. For **39**, the charge transfer events involving the  $\text{C}-\text{C}$  sigma bond as a donor are between  $\sigma(\text{C}-\text{C})$  and  $\sigma^*(\text{C}-\text{O})$  orbitals, where the overall value of  $\Delta E^{(2)}$  for this charge transfer event is 12.40 kcal/mol. Due to larger amounts of electron delocalisation between the  $\sigma(\text{C}-\text{C})$  and  $\sigma^*(\text{C}-\text{O})$  orbitals of **39**, **39** has a smaller



covalent C–C bond character, in contrast to **38**, which results in a longer and weaker C–C bond for **39** with respect to that of **38** (see Table 1).

### 3.4.7. CC strengths of a conjugated system

System **40** (Group 4) is a conjugated system consisting of a C=C, C–C, and C≡C bonds (see Figure 1). Generally, conjugated systems are said to possess stronger (more stable) single CC bonds due to some  $\pi$ -like bond character. From Table 1, we observe that the C–C bond of **40** is stronger than all C–C bonds of Group 3, where the difference between the BSO  $n(\text{C–C})$  of **40** and largest BSO  $n(\text{C–C})$  value of Group 3 (**30**) is 0.241 units. Comparing the energy density values at the C–C BCP,  $H_c$  of **30** and **40** shows that the C–C of **40** acquires a greater covalent character ( $-2.189 \text{ h}/\text{\AA}^3$  (**40**)). Note that the energy density value at the C–C BCP of the conjugated system (**40**) falls between the range of energy density values for the C=C systems of Group 2 and the C–C systems of Group 3; with regard to Group 3 this value is seen to range from  $-1.205$  to  $1.819$  and for Group 2 this value ranges from  $-3.018$  to  $-3.333 \text{ h}/\text{\AA}^3$ . These results demonstrate the  $\pi$ -like bond character of the C–C bond within **40**. From Table 1, we observe the C=C bond of **25** and **26** to be weaker than that of the conjugated system (**40**). Moreover, the C≡C bond of **40** is stronger than that of the weakest C≡C bond of Group 1 (**13**) (see Table 1).

## 4. Conclusion

Understanding how a substituent influences electronic rearrangement, and in turn, CC bond strength, is essential to the chemist as it enables one to classify molecules and to discover, categorise, and predict reaction mechanisms such as those involving CC bond cleavage. In this work, we investigated a set of 40 systems comprised of 3 parent structures, 36 hydrocarbon derivatives, and a conjugated system to comprehensively investigate the influence of various substituents on C≡C, C=C, and C–C bond strength.

We made use of local mode force constants, obtained via local vibrational mode analysis, to provide a quantitative bond strength measure for CC bonds. Electron density and NBO analyses were used to complement the results from local vibrational mode analysis. We established the covalent bond nature for every CC bond using the energy density  $H_c$  at the bond critical point  $r_c$  (BCP). Through this work the following was concluded:

- (1) The overall strongest and weakest C≡C bonds of Group 1 are for di-fluorinated [BSO  $n = 3.560$  (**3**)] and di-formylated acetylene [BSO  $n = 3.148$  (**13**)], respectively. With regard to Group 2, the

cis-1,2-fluorination of ethylene yields the strongest C=C bond [BSO  $n = 2.051$  (**15**)] while the trans-1,2-hydroxylation of ethylene results in the weakest C=C bond [BSO  $n = 1.673$  (**18**)]. Within Group 3, the strongest C–C bond is found within 1,2-dihydroxyethane [BSO  $n = 1.057$  (**30**)] and the weakest C–C bond is found from the 1,1,2,2-tetracarboxylation of ethane [BSO  $n = 0.789$  (**39**)].

- (2) By comparing CC triple, double, and single bonded analogs (e.g. comparing cis-/trans-configurations which acquire the same substituent), we observe the CC interactions to be weaker for the systems that involve a greater magnitude of electron delocalisation (i.e. hyperconjugation) to and/or from the CC bond region. The instances of hyperconjugation across systems differ as the substituents vary in their inductive and  $\sigma/\pi$  withdrawing/accepting nature.
- (3) From negative energy density values  $H_c$  taken at the bond critical point  $r_c$ , the covalent nature of all C≡C, C=C, and C–C bonds was confirmed. In a majority of instances  $H_c$  correlates with corresponding  $k^a$  or BSO  $n(\text{CC})$  measures revealing that the strengthening of C≡C, C=C, and C–C bonds occurs when the covalent nature of the bond increases. Although, we also find some notable anomalies: di-fluorinated acetylene (**3**), di-hydroxylated acetylene (**5**), di-aminated acetylene (**11**), di-carboxylated acetylene (**13**), trans-1,2-dihydroxyethylene (**18**), 1,1,2,2-tetrafluorinated ethane (**29**), and 1,1,2,2-tetracarboxylated ethane (**39**) (see Figure 4). These results show that the local mode force constant is a sensitive bond strength descriptor that takes into account second-order effects unlike the energy density which is analysed only at the bond critical point, where the  $k^a$  considers CC modulation via charge delocalisation (i.e. hyperconjugation effects), dispersion interactions, or steric repulsion effects.
- (4) It was observed that the C–C bond within the conjugated system (**40**) is stronger than any C–C bond of Group 3. The  $\pi$ -like character of the C–C bond within **40** was verified from the energy density  $H_c$  taken at the bond critical point  $r_c$  where the  $H_c$  value reveals that the covalent nature of the C–C bond within **40** is greater than that generally observed for the CC single bonded systems of Group 3 and is smaller than that of the CC double bonded systems of Group 2.

In general, this investigation demonstrates that the local mode force constant allows for one to comprehend how a substituent effects the electronic structure/nature of CC triple, double, and single bonds. We show that



the strengthening or weakening of these bonds is due to increasing/decreasing covalent bond character which becomes altered through charge transfer events that are dictated by the substituent in play. The local mode force constant is powerful in the sense that it can provide information to guide the fine-tuning of CC triple, double, and single bond strength.

## Acknowledgments

This work was supported by the National Science Foundation, Grant No. CHEM-2102461. The authors thank SMU for providing generous computational resources. VO thanks the São Paulo Research Foundation (FAPESP) for grant number 2018/13673-7.

## Disclosure statement

No potential conflict of interest was reported by the author(s).

## Funding

This work was supported by the National Science Foundation [grant number CHE 1464906]. VO thanks the São Paulo Research Foundation (FAPESP) [grant number 2018/13673-7].

## ORCID

Alexis Antoinette Ann Delgado  <http://orcid.org/0000-0002-6785-8023>

Daniel Sethio  <http://orcid.org/0000-0002-8075-1482>

Devin Matthews  <http://orcid.org/0000-0003-2795-5483>

Elfi Kraka  <http://orcid.org/0000-0002-9658-5626>

## References

- [1] S. Kanshio, *J. Pet. Sci. Eng.* 184, 1–13 (2020). doi:10.1016/j.petrol.2019.106590106590.
- [2] V. Litvinenko, *Resources* 9 (59), 1–22 (2020). doi:10.3390/resources9050059.
- [3] R. Mülhaupt, *Macromol. Chem. Phys.* 214 (2), 159–174 (2012). doi:10.1002/macp.201200439
- [4] M.S. Qureshi, A. Oasmaa, H. Pihkola, I. Deviatkin, A. Tenhunen, J. Mannila, H. Minkkinen, M. Pohjakallio and J. Laine-Ylijoki, *J. Anal. Appl. Pyrolysis* 152, 1–11 (2020). doi:10.1016/j.jaap.2020.104804104804.
- [5] N. Sivaram, P. Gopal and D. Barik, *Chapter 4 – Toxic Waste From Textile Industries* (Woodhead Publishing, Cambridge, 2019).
- [6] H. Wilkes and J. Schwarzbauer, in *Handbook of Hydrocarbon and Lipid Microbiology*, edited by Kenneth N. Timmis (Springer, Berlin, Heidelberg, 2010), pp. 1–48.
- [7] B. Rybtchinski and D. Milstein, *Angew. Chem. Int. Ed.* 38 (7), 870–883 (1999). doi:10.1002/(ISSN)1521-3773
- [8] I. Marek, A. Masarwa, P.O. Delaye and M. Leibel, *Angew. Chem. Int. Ed.* 54 (2), 414–429 (2014). doi:10.1002/anie.201405067
- [9] D.Y. Lee, B.S. Hong, E.G. Cho, H. Lee and C.H. Jun, *J. Am. Chem. Soc.* 125 (21), 6372–6373 (2003). doi:10.1021/ja034337n
- [10] C. Kyung-Mi, E.A. Jo and C.H. Jun, *Synlett* 2009 (18), 2939–2942 (2009). doi:10.1055/s-0029-1218000
- [11] Y. Gu, L. Ye, F. Lin, Y. Lin, T. Tang and L. Ma, *Polymer* 170, 24–30 (2019). doi:10.1016/j.polymer.2019.03.007
- [12] Y.J. Park, B.I. Kwon, J.A. Ahn, H. Lee and C.H. Jun, *J. Am. Chem. Soc.* 126 (43), 13892–13893 (2004). doi:10.1021/ja045789i
- [13] C.H. Jun, C.W. Huh and S.J. Na, *Angew. Chem. Int. Ed.* 37, 145–147 (1998). doi:10.1002/(ISSN)1521-3773
- [14] Y. Zhou, C. Rao, S. Mai and Q. Song, *J. Org. Chem.* 81 (5), 2027–2034 (2016). doi:10.1021/acs.joc.5b02887
- [15] K. Chen, G. Walker and N. Allinger, *J. Mol. Struct.: THEOCHEM* 490 (1–3), 87–107 (1999). doi:10.1016/S0166-1280(99)00079-2
- [16] J.E. Huheey, *J. Phys. Chem.* 69 (10), 3284–3291 (1965). doi:10.1021/j100894a011
- [17] L. Pauling, *J. Am. Chem. Soc.* 53 (4), 1367–1400 (1931). doi:10.1021/ja01355a027
- [18] J.A. Pople and M. Gordon, *J. Am. Chem. Soc.* 89 (17), 4253–4261 (1967). doi:10.1021/ja00993a001
- [19] M.T. Krygowski, *Chem. Rev.* 105 (10), 3482–3512 (2005). doi:10.1021/cr030081s
- [20] D.T. Clark, J.N. Murrell and J.M. Tedder, *J. Am. Chem. Soc.* 1250–1253 (1963). doi:10.1039/jr9630001250
- [21] O. Exner, *J. Phys. Org. Chem.* 12 (4), 265–274 (1999). doi:10.1002/(ISSN)1099-1395
- [22] B.K. Mishra, S. Karthikeyan and V. Ramanathan, *J. Chem. Theory Comput.* 8 (6), 1935–1942 (2012). doi:10.1021/ct300100h
- [23] D. Streets, *Chem. Phys. Lett.* 28 (4), 555–558 (1974). doi:10.1016/0009-2614(74)80103-X
- [24] S. Marriott, W.F. Reynolds, R.W. Taft and R.D. Topsom, *J. Org. Chem.* 49 (6), 959–965 (1984). doi:10.1021/jo00180a002
- [25] H. Ali, *Reaction Mechanism in Organic Chemistry* (S. Chand Publishing, New Delhi, India, 2016).
- [26] A.M. James, C.J. Laconsay and J.M. Galbraith, *J. Phys. Chem. A* 121 (27), 5190–5195 (2017). doi:10.1021/acs.jpca.7b02988
- [27] I.V. Alabugin, G. dos Passos Gomes and M.A. Abdo, *WIREs Comput. Mol. Sci.* 9 (2), 1389–1455 (2018). doi:10.1002/wcms.1389.
- [28] J.I.C. Wu and P. von Ragué Schleyer, *Pure Appl. Chem.* 85 (5), 921–940 (2013). doi:10.1351/PAC-CON-13-01-03
- [29] K.B. Wiberg and P.R. Rablen, *J. Am. Chem. Soc.* 115 (2), 614–625 (1993). doi:10.1021/ja00055a034
- [30] I.V. Alabugin, K.M. Gilmore and P.W. Peterson, *Wiley Interdiscip. Rev. Comput. Mol. Sci.* 1 (1), 109–141 (2011). doi:10.1002/wcms.v1.1
- [31] T.M. Krygowski and S.J. Grabowski, *Chem. Phys. Lett.* 389 (1–3), 51–57 (2004). doi:10.1016/j.cplett.2004.03.061
- [32] N.L. Allinger, L. Schäfer, K. Siam, V.J. Klimkowski and C.V. Alsenoy, *J. Comput. Chem.* 6 (5), 331–342 (1985). doi:10.1002/jcc.540060502
- [33] G. Glockler, *J. Chem. Phys.* 21 (7), 1242–1248 (1953). doi:10.1063/1.1699175
- [34] S.J. Grabowski, M.A. Walczak and T.M. Krygowski, *Chem. Phys. Lett.* 400 (4–6), 362–367 (2004). doi:10.1016/j.cplett.2004.10.130

- [35] K.B. Wiberg, M.A. Murcko, K.E. Laidig and P.J. MacDougall, *J. Phys. Chem.* 94 (18), 6956–6959 (1990). doi:10.1021/j100381a008
- [36] H. Lee, J.H. Baraban, R.W. Field and J.F. Stanton, *J. Phys. Chem. A.* 117, 11679–11683 (2013). doi:10.1021/jp400035a
- [37] K.B. Wiberg and P.R. Rablen, *J. Am. Chem. Soc.* 115 (20), 9234–9242 (1993). doi:10.1021/ja00073a044
- [38] K.B. Wiberg, C.M. Hadad, P.R. Rablen and J. Cioslowski, *J. Am. Chem. Soc.* 114 (22), 8644–8654 (1992). doi:10.1021/ja00048a044
- [39] E.A. Carter and W.A. Goddard, *J. Phys. Chem.* 90 (6), 998–1001 (1986). doi:10.1021/j100278a006
- [40] P. Furet, G. Hallak, R.L. Matcha and R. Fuchs, *Can. J. Chem.* 63, 2990–2994 (1985). doi:10.1139/v85-496
- [41] N. Laurencelle and P.D. Pacey, *J. Am. Chem. Soc.* 115 (2), 625–631 (1993). doi:10.1021/ja00055a035
- [42] M.W. Schmidt, P.N. Truong and M.S. Gordon, *J. Am. Chem. Soc.* 109, 5217–5227 (1987). doi:10.1021/ja00251a029
- [43] O. Travnikova, S. Svensson, D. Céolin, Z. Bao and M.N. Piancastelli, *Phys. Chem. Chem. Phys.* 11, 826–833 (2009). doi:10.1039/B805912H
- [44] J. Berkowitz, C.A. Mayhew and B. Rušćić, *J. Chem. Phys.* 88 (12), 7396–7404 (1988). doi:10.1063/1.454352
- [45] K.B. Wiberg, R.F.W. Bader and C.D.H. Lau, *J. Am. Chem. Soc.* 109 (4), 1001–1012 (1987). doi:10.1021/ja00238a005
- [46] J.D. Dill, A. Greenberg and J.F. Liebman, *J. Am. Chem. Soc.* 101 (23), 6814–6826 (1979). doi:10.1021/ja00517a005
- [47] E. Ploshnik, D. Danovich, P.C. Hiberty and S. Shaik, *J. Chem. Theory Comput.* 7 (4), 955–968 (2011). doi:10.1021/ct100741b
- [48] K.B. Wiberg and K.E. Laidig, *J. Org. Chem.* 57 (19), 5092–5101 (1992). doi:10.1021/jo00045a019
- [49] O. Exner and S. Böhm, *J. Comput. Chem.* 25 (16), 1979–1986 (2004). doi:10.1002/jcc.v25:16
- [50] H. Maskill, *The Physical Basis of Organic Chemistry (Oxford Science Publications)* (Oxford University Press, Oxford, England, 1986).
- [51] G.R.S. de Freitas and C.L. Firme, *J. Mol. Model* 19 (12), 5267–5276 (2013). doi:10.1007/s00894-013-2022-6
- [52] N. Jayakumar, P. Kolandaivel, N. Kuze, T. Sakasumi and O. Ohashi, *J. Mol. Struct.: THEOCHEM* 465 (2–3), 197–202 (1999). doi:10.1016/S0166-1280(98)00336-4
- [53] I.V. Alabugin and S.B.M. Manoharan, *J. Phys. Chem. A.* 118 (20), 3663–3677 (2014). doi:10.1021/jp502472u
- [54] I.V. Alabugin, M. Manoharan, S. Peabody and F. Weinhold, *J. Am. Chem. Soc.* 125 (19), 5973–5987 (2003). doi:10.1021/ja034656e
- [55] I.V. Alabugin and M. Manoharan, *J. Comput. Chem.* 28 (1), 373–390 (2006). doi:10.1002/(ISSN)1096-987X
- [56] R.G. Parr and R.G. Pearson, *J. Am. Chem. Soc.* 105 (26), 7512–7516 (1983). doi:10.1021/ja00364a005
- [57] R.G. Pearson, *J. Org. Chem.* 54 (6), 1423–1430 (1989). doi:10.1021/jo00267a034
- [58] Y. Apeloig, *J. Chem. Soc. Chem. Comm.* 1 (9), 396 (1981). doi:10.1039/c39810000396
- [59] G.J. Martin, M.L. Martin and S. Odiod, *Org. Magn. Reson.* 7 (1), 2–17 (1975). doi:10.1002/(ISSN)1097-458X
- [60] L.A. Curtiss and J.A. Pople, *J. Chem. Phys.* 88 (12), 7405–7409 (1988). doi:10.1063/1.454303
- [61] J.E. Huheey, *J. Org. Chem.* 31 (7), 2365–2368 (1966). doi:10.1021/jo01345a067
- [62] K.B. Wiberg, C.M. Hadad, T.J. LePage, C.M. Breneman and M.J. Frisch, *J. Phys. Chem.* 96 (2), 671–679 (1992). doi:10.1021/j100181a030
- [63] M.D. Newton and W.N. Lipscomb, *J. Am. Chem. Soc.* 89 (17), 4261–4267 (1967). doi:10.1021/ja00993a002
- [64] N. Muller and D.E. Pritchard, *J. Chem. Phys.* 31 (26), 1471–1476 (1959). doi:10.1063/1.1730638
- [65] R. Trambarulo and W. Gordy, *J. Chem. Phys.* 18 (12), 1613–1616 (1950). doi:10.1063/1.1747549
- [66] H.A. Bent, *Chem. Rev.* 61 (3), 275–311 (1961). doi:10.1021/cr60211a005
- [67] H.D. Thomas, K. Chen and N.L. Allinger, *J. Am. Chem. Soc.* 116 (13), 5887–5897 (1994). doi:10.1021/ja00092a045
- [68] S.W. Benson and M. Luria, *J. Am. Chem. Soc.* 97 (4), 704–709 (1975). doi:10.1021/ja00837a004
- [69] D. Cremer and E. Kraka, *Angew. Chem. Int. Ed.* 23, 627–628 (1984). doi:10.1002/(ISSN)1521-3773
- [70] D. Cremer, A. Wu, J.A. Larsson and E. Kraka, *J. Mol. Model.* 6, 396–412 (2000). doi:10.1007/PL00010739
- [71] D. Cremer, J.A. Larsson and E. Kraka, in *Theoretical and Computational Chemistry*, edited by C. Parkanyi (Elsevier, Amsterdam, 1998), pp. 259–327.
- [72] D. Cremer and E. Kraka, *Croatica Chem. Acta.* 57, 1259–1281 (1984).
- [73] E. Kraka and D. Cremer, *Rev. Proc. Quim.* 39–42 (2012).
- [74] R.F.W. Bader, T.H. Tang, Y. Tal and F.W. Biegler-Koenig, *J. Am. Chem. Soc.* 104 (4), 946–952 (1982). doi:10.1021/ja00368a004
- [75] R.F.W. Bader, *Atoms in Molecules: A Quantum Theory* (Oxford University Press, Oxford, England, 1994).
- [76] Z. Konkoli and D. Cremer, *Int. J. Quantum Chem.* 67, 1–9 (1998). doi:10.1002/(ISSN)1097-461X
- [77] Z. Konkoli, J.A. Larsson and D. Cremer, *Int. J. Quantum Chem.* 67, 11–27 (1998). doi:10.1002/(ISSN)1097-461X
- [78] W. Zou, R. Kalescky, E. Kraka and D. Cremer, *J. Chem. Phys.* 137, 1–11 (2012). doi:10.1063/1.4747339
- [79] E. Kraka, W. Zou and Y. Tao, *WIREs: Comput. Mol. Sci.* 10, 1–34 (2020). doi:10.1002/wcms.1480
- [80] W. Zou and D. Cremer, *Chem. Eur. J.* 22, 4087–4097 (2016). doi:10.1002/chem.v22:12
- [81] Y. Tao, W. Zou, D. Cremer and E. Kraka, *J. Phys. Chem. A.* 121, 8086–8096 (2017). doi:10.1021/acs.jpca.7b08298
- [82] R. Kalescky, E. Kraka and D. Cremer, *Int. J. Quantum Chem.* 114, 1060–1072 (2014). doi:10.1002/qua.v114:16
- [83] R. Kalescky, W. Zou, E. Kraka and D. Cremer, *J. Phys. Chem. A.* 118, 1948–1963 (2014). doi:10.1021/jp4120628
- [84] A. Humason, W. Zou and D. Cremer, *J. Phys. Chem. A.* 119, 1666–1682 (2014). doi:10.1021/jp5082966
- [85] A.A.A. Delgado, A. Humason, R. Kalescky, M. Freindorf and E. Kraka, *Molecules* 26 (4), 1–24 (2021). doi:10.3390/molecules26040950950
- [86] G.D. Purvis and R.J. Bartlett, *J. Chem. Phys.* 76 (4), 1910–1918 (1982). doi:10.1063/1.443164

- [87] J.A. Pople, M. Head-Gordon and K. Raghavachari, *J. Chem. Phys.* 87 (10), 5968–5975 (1987). doi:10.1063/1.453520
- [88] T.H. Dunning, *J. Chem. Phys.* 90 (2), 1007–1023 (1989). doi:10.1063/1.456153
- [89] R.A. Kendall, T.H. Dunning and R.J. Harrison, *J. Chem. Phys.* 96, 6796–6806 (1992). doi:10.1063/1.462569
- [90] J.F. Stanton, J. Gauss, L. Cheng, M.E. Harding, D.A. Matthews and P.G. Szalay, *CFOUR, Coupled-Cluster Techniques for Computational Chemistry, A Quantum-Chemical Program Package*. <http://www.cfour.de> (accessed Aug 10, 2019).
- [91] D.A. Matthews, L. Cheng, M.E. Harding, F. Lipparini, S. Stopkowitz, T.C. Jagau, P.G. Szalay, J. Gauss and J.F. Stanton, *J. Chem. Phys.* 152 (21), 1–35 (2020). doi:10.1063/5.0004837214108.
- [92] J. Gauss and J.F. Stanton, *Chem. Phys. Lett.* 276, 70–77 (1999). doi:10.1016/S0009-2614(97)88036-0
- [93] J.F. Stanton and J. Gauss, *Inter. Rev. Phys. Chem.* 19, 61–95 (2000). doi:10.1080/014423500229864
- [94] W. Zou, Y. Tao, M. Freindorf, M.Z. Makoś, N. Verma and E. Kraka, *Local Vibrational Mode Analysis (LMoDeA)* (Computational and Theoretical Chemistry Group (CATCO), Southern Methodist University, Dallas, TX, USA, 2020).
- [95] E.B. Wilson, J.C. Decius and P.C. Cross, *Molecular Vibrations. The Theory of Infrared and Raman Vibrational Spectra* (McGraw-Hill, New York, 1955).
- [96] Z. Konkoli and D. Cremer, *Int. J. Quantum Chem.* 67, 29–40 (1998). doi:10.1002/(ISSN)1097-461X
- [97] Z. Konkoli, J.A. Larsson and D. Cremer, *Int. J. Quantum Chem.* 67, 41–55 (1998). doi:10.1002/(ISSN)1097-461X
- [98] D. Cremer and E. Kraka, *Curr. Org. Chem.* 14, 1524–1560 (2010). doi:10.2174/138527210793563233
- [99] E. Kraka, J.A. Larsson and D. Cremer, in *Computational Spectroscopy*, edited by J. Grunenberg (Wiley, New York, 2010), pp. 105–149.
- [100] F. Weinhold and C.R. Landis, *Valency and Bonding: A Natural Bond Orbital Donor-Acceptor Perspective* (Cambridge University Press, Cambridge, England, 2005).
- [101] A.E. Reed, L.A. Curtiss and F. Weinhold, *Chem. Rev.* 88 (6), 899–926 (1988). doi:10.1021/cr00088a005
- [102] E.D. Glendening, J.K. Badenhoop, A.E. Reed, J.E. Carpenter, J.A. Bohmann, C.M. Morales, C.R. Landis and F. Weinhold, NBO6 2013, Theoretical Chemistry Institute, University of Wisconsin, Madison.
- [103] T.A. Keith, *TK Gristmill Software* ([aim.tkgristmill.com](http://aim.tkgristmill.com)).
- [104] E. Kraka and D. Cremer, in *Theoretical Models of Chemical Bonding. The Concept of the Chemical Bond*, Vol. 2 (Z.B. Maksic, ed., Springer Verlag, Berlin, Heidelberg, 1990), pp. 453–542.
- [105] D. Setiawan, D. Sethio, D. Cremer and E. Kraka, *Phys. Chem. Chem. Phys.* 20 (1), 23913–23927 (2018). doi:10.1039/C8CP03843K
- [106] C. Andrew, E.E. Etim, O.A. Ushie and G.P. Khanal, *Chem. Sci. Trans.* 7 (1), 77–82 (2018). doi:10.7598/cst2018.1432.
- [107] G. Herzberg, *Electronic Spectra and Electronic Structure of Polyatomic Molecules* (Van Nostrand, New York, NY, 1966).
- [108] J.A. Bell, *Chemistry: A Project of the American Chemical Society* (W H Freeman 'I&' CO, New York, NY, 2004).
- [109] R. Kalescky, E. Kraka and D. Cremer, *J. Phys. Chem. A.* 117, 8981–8995 (2013). doi:10.1021/jp406200w
- [110] M. Kaupp, D. Danovich and S. Shaik, *Coord. Chem. Rev.* 344, 355–362 (2017). doi:10.1016/j.ccr.2017.03.002
- [111] M. Kaupp, B. Metz and H. Stoll, *Angew. Chem. Int. Ed.* 39 (24), 4607–4609 (2000). doi:10.1002/(ISSN)1521-3773
- [112] D.S. Kemp and F. Vellaccio, *Organic Chemistry* (Worth Publishers, New York, NY, 1980).
- [113] D. Banerjee, A. Ghosh, S. Chattopadhyay, P. Ghosh and R.K. Chaudhuri, *Mol. Phys.* 112 (24), 3206–3224 (2014). doi:10.1080/00268976.2014.938710